

MagicClay: Sculpting Meshes With Generative Neural Fields

AMIR BARDA, Tel Aviv University, Israel
 VLADIMIR G. KIM, Adobe Research, USA
 NOAM AIGERMAN, Université de Montréal, Canada
 AMIT H. BERMANO, Tel Aviv University, Israel
 THIBAUT GROUEIX, Adobe Research, USA

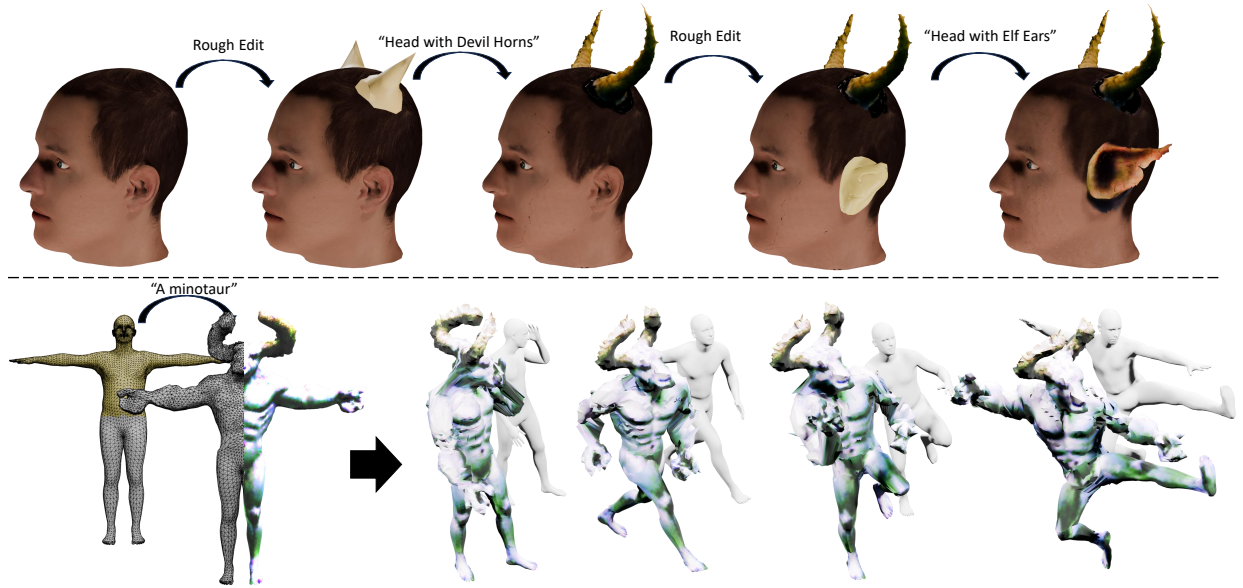


Fig. 1. *Top*: the user selects a region of an input mesh, coarsely sketches the intended edit, inputs a text-prompt, and MagicClay grows the region automatically to match the prompt, while the rest of the shape and existing textures remain unchanged, and the mesh remains topologically valid (no non-manifold edges or vertices). Importantly, due to working directly on the input mesh, these edits can be made sequentially. *Bottom*: MagicClay preserves attributes from the input mesh such as texture, rig, and tessellation, e.g. allowing to transfer an animation from source to edited shape.

The recent developments in neural fields have brought phenomenal capabilities to the field of shape generation, but they lack crucial properties, such as incremental control – a fundamental requirement for artistic work. Triangular meshes, on the other hand, are the representation of choice for most geometry-related tasks, offering efficiency and intuitive control, but do not lend themselves to neural optimization. To support downstream tasks, previous art typically proposes a two-step approach, where first, a shape is generated using neural fields, and then a mesh is extracted for further processing. Instead, in this paper, we introduce a hybrid approach that maintains both a mesh and a Signed Distance Field (SDF) representations consistently. Using this representation, we introduce MagicClay – a tool for sculpting regions of a mesh according to textual prompts while keeping other regions untouched. Our method is designed to be compatible with existing mesh sculpting workflows. The user sculpts the desired shape using the existing brushes and our pipeline then evolves the geometry and triangulation of the selected mesh part according to the given textual prompt. This process operates on the original mesh while preserving its meta-data. Our framework carefully and efficiently balances consistency between the representations and regularizations in every step of the shape optimization. Relying on the

mesh representation, we show how to render the SDF at higher resolutions and faster. In addition, we employ recent work in differentiable mesh reconstruction to adaptively allocate triangles in the mesh where required, as indicated by the SDF. Using an implemented prototype, we demonstrate superior generated geometry compared to the state-of-the-art and novel consistent control, allowing sequential prompt-based edits to the same mesh for the first time. We will release the code upon acceptance.

1 INTRODUCTION

The field of 3D shape generation has always been heavily dependent on the representations it uses for the shapes. Recent neural field-based representations (i.e., NeRFs [Mildenhall et al. 2020] or SDFs [Park et al. 2019; Chen and Zhang 2019]), have shown remarkable progress to the task [Poole et al. 2023; Wang et al. 2023a] in a very short time. These representations are robust to noisy losses and are naturally well-suited for neural frameworks, yielding impressive results and avoiding local minima. On the other hand, these representations are expensive to evaluate (limited by volumetric rendering resolutions) and lack acutely in geometric control, such as allowing users to localize their edits or leverage surface-based (e.g., smoothness) priors. For instance, when iterating on a design

Authors' addresses: Amir Barda, amirbarda@mail.tau.ac.il, Tel Aviv University, Israel; Vladimir G. Kim, Adobe Research, USA; Noam Aigerman, Université de Montréal, Canada; Amit H. Bermano, Tel Aviv University, Israel; Thibault Groueix, Adobe Research, USA.

of a mesh-based 3D model, as artists alter geometry, textures, or topology, they expect any additional updates to retain previously assigned attributes. This level of control is currently not feasible with the neural field-based representations.

In contrast, triangular meshes provide such control and are indeed the current dominant representation for most 3D applications in the industry, as they are computationally inexpensive, consistent, and intuitive. On the other hand, while the adaptive, non-uniform nature of meshes is one of their greatest advantages, it is also the reason they are not widely used in current generative frameworks. The sparse gradients induced by meshes tend to limit the ability of optimizations to achieve large deformations in a stable manner.

For this reason, many works [Lin et al. 2023] turn to a two-step process, where first implicit functions are used for coarse generation, and then are converted to meshes in a second step for the purpose of finer details or downstream editability. However, as we demonstrate, two-stage pipelines are prone to local minima and cannot be extended to the task of editing an existing mesh with pre-existing UVs and textures, for example.

In this paper, we present MagicClay - a shape editing framework based on a hybrid implicit-explicit representation. MagicClay optimizes an input mesh (possibly textured) and its SDF jointly at every step of the generation process and leverages consistency and representation-specific priors, benefiting from the best of both worlds. This approach leads to higher quality generation output and also enables a higher level of control, allowing the users to sequentially sculpt local generative details in regions marked as editable, guided by the user-provided prompt. Sculpting is a common approach used in 3D modeling software [Blender 2024; ZBrush 2024; SubstanceModeler 2024]. While sculpting currently requires a lot of time and expertise, our novel tool offers unprecedented control by allowing artists to select a region on a mesh to be modified, provide a textual prompt, and hallucinate an updated region (Figure 1).

The key technical challenge of the hybrid approach is keeping the two representations synced efficiently. To achieve this, we differentially render both representations from various angles and require consistency in RGB renders, opacity, and normal maps. Furthermore, we rely on the in-sync-mesh representation to render the SDF at higher resolutions and faster; instead of the hundreds of samples per ray required in most previous techniques [Poole et al. 2023], we localize the SDF sampling around the mesh surface and use as little as three samples. Critically, optimizing a mesh consistently and stably is an additional challenge. In terms of resolution, a coarse mesh would not be expressive enough for novel details, and a fine mesh is expensive and unstable. Hence, an adaptive tessellation is required, that changes along with the shape where needed. We rely on recent developments in differentiable mesh reconstruction [Barda et al. 2023] to achieve dynamic mesh topology updates, including face splitting, edge collapse, and edge flips. To texture the mesh despite changes in its topology, we contribute a new strategy based on triangle supersampling. Importantly, using this layer, we can maintain mesh properties (e.g. vertex groups for animation) throughout the optimization, and through local mesh topology changes.

As we demonstrate, our hybrid approach allows localized and sequential mesh editing operations, allowing the user to preserve existing mesh triangulation and information in some regions, while

allowing radical and semantic changes in other regions. In addition, we show overall higher generated geometric quality as compared to using an implicit representation alone, thanks to the priors the two representations impose on each other. By combining the merits of implicit and explicit representations to enable a novel generative sculpting tool, we bring the neural shape generation pipeline closer to the artistic workflows, allowing for incremental editing steps and providing the artist with precision and control over the end result.

To summarize, our main contributions are :

- A new hybrid representation that brings the benefits of SDFs and meshes together : SDFs are more robust to noisy gradients (see Figure 3) and meshes allow for surface-based losses and localization of edits. Both representations are kept consistent via multi-view consistency losses and adaptive remeshing. In Figure 4 and Table 1, we demonstrate in the task of unconditional text-to-3D that MagicClay produces higher-quality meshes than other representations using similar generative techniques.
- An application of the new representation to localized mesh editing, which brings the prowess of generative techniques to mesh sculpting, while critically preserving the part of the geometry that is *not* selected for editing, including its texture, tessellation, and rigging parameters. We show in Figure 8 that our method produces higher-quality and more localized edits than competing methods.

2 RELATED WORK

Unconditional 3D generative models. In their seminal work, DreamFusion, [Poole et al. 2023] show that Text-to-Image diffusion models can be used to provide gradients to optimize a Neural Radiance Field (NeRF) via Score Distillation Sampling (SDS). Magic3D [Lin et al. 2023] achieves better quality by using a two-stage approach: the first stage is similar to DreamFusion, and they note that the quality of the generated object is limited by the high cost of performing volumetric rendering for high-resolution images. The second stage uses a differentiable mesh representation to refine the generated object further, as differentiable rendering meshes in high resolution is significantly cheaper in both time and memory. Magic123 [Qian et al. 2024] further improves upon Magic3D by using both 3D and 2D diffusion priors. ProlificDreamer [Wang et al. 2023a] proposes an improvement over SDS, the VSD loss, to drive 3D generation from 2d diffusion priors. Fantasia3D [Chen et al. 2023] and TextMesh [Tsalicoglou et al. 2024] decouple the appearance from the geometry by replacing the NeRF with an SDF, and optimizing a color network separately. TextDeformer [Gao et al. 2023] uses CLIP as prior together with a novel gradient smoothing technique based on mesh Jacobians to deform meshes according to a text prompt.

The choice of using two stages in Magic3D [Lin et al. 2023] highlights the tradeoffs involved in choosing the right representation for 3D generative models. While implicit functions are well suited for coarse generation because they allow topology updates, meshes can be rasterized very efficiently at a high resolution to get fine details in a second step. However, two-stage pipelines are prone to local minima and crucially, cannot be extended to edit an existing mesh with pre-computed UVs. In contrast, we jointly optimize a

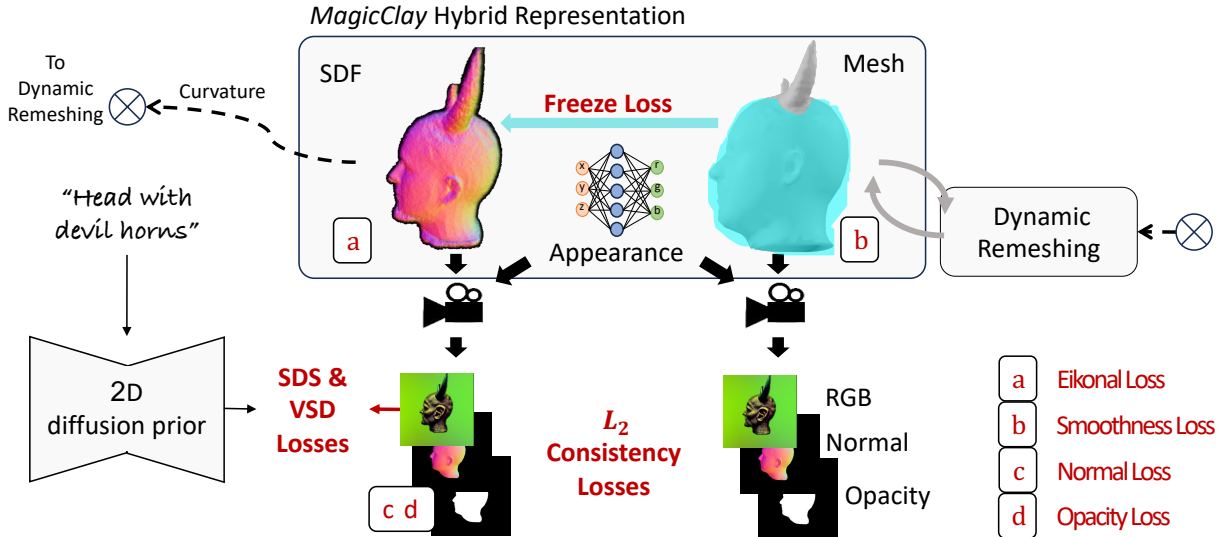


Fig. 2. **Overview of the hybrid optimization.** We jointly optimize a mesh, an SDF and a shared appearance MLP according to an input prompt. We can either optimize the full geometry, or only a user-selected portion of the mesh for an iterative 3D modeling workflow. We can also preserve existing textures on non-selected part of the mesh, or have the diffusion model generate textures for the full mesh. We start by differentially rendering both representations, and enforcing their consistency. As they are kept in sync, we use the mesh to efficiently sample volumetric rays to render hi-res maps from the SDF in a memory-efficient manner. Applying SDS-type losses on these Hi-res renderings allows for capturing finer details. We sync the mesh and the SDF via multi-view consistency constraints on the RGB pixels, the image opacity, and the surface normals. The mesh local topology is updated according to the SDF using ROAR [Barda et al. 2023], splitting triangles where geometry is created and collapsing edges where needed. Additionally, we leverage representation-specific losses to regularize the optimization: an Eikonal loss on the SDF and a smoothness loss on the mesh.

hybrid SDF and mesh representation, that can be initialized from an existing mesh and maintain all of its properties during optimization, benefiting from the best of both worlds in a *1-step pipeline*: topology updates from the SDF part and fine details from the mesh part.

Finally, Instant3D [Li et al. 2024] generates a 3D shape in a single forward pass without requiring any costly optimization. Though faster and higher-quality, Instant3D does not allow sculpting an existing mesh like MagicClay.

Generative local editing. A recent line of work deals with locally editing a 3D scene. Unlike 2D images, selecting a region in 3D to be edited is not straightforward for implicit functions. Most of these works solely rely on soft attention between the text and the renderings to semantically understand the area to be edited, and they vary with their choice of 3D representation. Vox-E [Sella et al. 2023] and DreamEditor [Zhuang et al. 2023] encode an SDF respectively with a voxel grid and an MLP. Instruct-NerftoNerf [Haque et al. 2023], LatentNerf [Metzer et al. 2023], SKED [Mikaeili et al. 2023], MVEdit [Chen et al. 2024] use a NeRF. In these methods, the user selects the region to edit via the prompt, except for SKED [Mikaeili et al. 2023], which additionally utilizes guiding sketches from different views. FocalDreamer [Li et al. 2023] and Progressive3D [Cheng et al. 2024] use an implicit representation with SDS and additionally allow selection of 3D region(s) with losses encouraging localized changes. The output mesh is reconstructed from the edited SDF using DMTeT, thus losing all mesh properties in the non-editable regions. In contrast, our method exposes a mesh to the user, on which it is trivial to select a region and guarantees that the unselected part

will be unaltered.

Hybrid Representations. Unlike for 2D images, there is no ubiquitous representation in 3D, and several representations exist and have been combined for diverse 3D tasks, suggesting that there is no one-fit-for-all solution. In this work, we introduce a hybrid representation specialized for generative modeling and focus the related work on hybrids most relevant to this paper. [Poursaeed et al. 2020] uses a coupling of implicit and explicit surface representations for generative 3D modeling, kept in sync by 3D losses. NerfMeshing [Rakotosaona et al. 2024] proposes an improved meshing pipeline for NeRFs. Finally, DmTeT [Shen et al. 2021] proposes deep marching Tetrahedra as a hybrid representation for high-resolution 3D Shape synthesis, notably used in the concurrent work Magic3D [Lin et al. 2023]. Our method uses both a set of regularization losses, as well as a dynamic projection layer based on ROAR [Barda et al. 2023] to keep the SDF and mesh part in sync.

Traditional approaches for sculpting meshes Many commercial tools employ the digital sculpting metaphor for 3D modeling, such as Zbrush [ZBrush 2024], Mudbox [Autodesk 2024], or SubstanceModeler [SubstanceModeler 2024]. Motivated by these workflows, geometry processing research has focused on improving interactive techniques such as mesh deformation [Jacobson et al. 2014], mesh blending for cut-and-paste [Biermann et al. 2002], local parameterization for adding surface details [Schmidt et al. 2006], symmetry-guided autocompletion [Peng et al. 2018], and version

control for collaborative editing [Salvati et al. 2015]. Despite these advances, 3D modeling remains only accessible to experts. As an alternative, example-based approaches propose to democratize 3D modeling tools by using existing geometry from a database of stock 3D models to assemble new shapes from parts [Funkhouser et al. 2004]. Subsequent methods have built statistical models over part assemblies [Kalogerakis et al. 2012], and allow semantic control for deformations [Yumer et al. 2015]. Despite their accessibility, these tools are often restricted in their domain, and rely on heavy annotation of 3D assets, and thus have received limited use by professional modelers. In this paper, we utilize pre-trained 2D generative data priors to enable semantic controls for local and iterative modeling workflow without the need for pre-annotated 3D data.

3 METHOD

Given a mesh, a user-highlighted surface region, and a text prompt that describes the desired target, MagicClay optimizes the shape of the selected region so that the resulting mesh matches the target. To drive the shape optimization, we follow current literature and use the Score Distillation Sampling (SDS) technique [Poole et al. 2023] with differentiable rendering to leverage on text-conditioned 2D diffusion and guide the shape optimization. This approach, however, does not perform well when operated on meshes. Meshes are driven by sparse and irregular samples (vertices), and their connectivity mandates a stable and smooth deformation, avoiding self-intersections and flip-overs. For this reason, we employ a neural Signed Distance Field (SDF) to drive the mesh shape optimization and topology updates. We thus propose a hybrid representation that captures both a Signed Distance Field (SDF) and the surface, gaining from the advantages of both worlds. While the SDF allows guiding the shape toward larger-scale complex changes, the mesh allows localized control of the user-highlighted surface region.

In this section, we provide details on the hybrid SDF/Mesh representations (Sec. 3.1), how it can be efficiently optimized with SDS guidance (Sec. 3.2), how to effectively use surface and volumetric priors (Sec. 3.3), and how to update the mesh topology during optimization (Sec. 3.4). Figure 2 overviews the full pipeline.

3.1 Hybrid Representation

Our hybrid representation consists of a surface (a mesh), a volume (an SDF), and a shared appearance network encoding RGB colors for an input 3D coordinate. Both the surface and the volumetric representations can be differentially rendered, leveraging the shared appearance network to output images with color, normals, and opacity channels. We now detail these three elements.

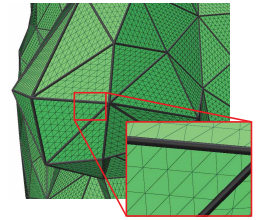
Surface Representation. We represent the surface of the shape as a 2-manifold triangular mesh. Mesh topology, or sampling resolution, is locally adapted according to the SDF (see Sec. 3.4 for details). We encode colors for the editable areas of the mesh using an auxiliary appearance network, derived from the SDF itself (see below). We found this approach simpler and more natural than traditional mesh coloring techniques; Using per-vertex colors is sensitive to triangulation, and would require a large number of vertices to match the resolution of the SDF. Using a texture image requires a complex UV parameterization, usually done a priori on a fixed shape.

In addition, our surface is continuously optimized and undergoes topological changes, re-tessellation, and large-scale deformations, which makes it computationally infeasible to apply traditional UV parameterization techniques during this optimization.

Instead, our hybrid approach offers a simpler approach to shape coloring. To apply the colors from the appearance network to the mesh, we propose to adaptively subdivide each face of the base mesh according to the triangle area.

Since we only use these subdivided triangles to represent colors, they do not have to form a connected mesh, unlike traditional subdivision techniques. Thus, we employ the MeshColors scheme that was initially proposed for UV-less texturing [Yuksel et al. 2010] and has an efficient GPU implementation.

In the inset, we illustrate the example subdivision; note how sub-triangles on two adjacent faces do not share the vertices along the edge. During rendering, we assign a color to each sub-triangle by interpolating the colors at its three vertices. These are obtained by querying the appearance network at the super-sampled vertices location.. We find that this approach strikes a balance between a compact low-poly representation for flat parts of the generated surface, while still allowing for high-frequency textures.



Signed Distance Functions. Our volumetric shape representation is chosen off-the-shelf, and conceptually serves as a regularization guiding the mesh changes using existing state-of-the-art text2shape tools. We use a continuous scalar field that can be sampled anywhere in \mathbf{R}^3 , returning a signed shortest distance to the surface (negative on the inside, positive on the outside). We encode the SDF using a multiresolution hash encoding of features defined over a grid which are then mapped to distance value by a small MLP, following instant-NGP [Müller et al. 2022]. As in the mesh case, the shared appearance network is sampled to obtain colors during rendering.

Appearance Network. The shared appearance network encodes colors implicitly as a map over \mathbf{R}^3 . It shares the same hash grid as the SDF, but has a smaller MLP head, with a single hidden layer that take hash grid features as input and outputs RGB values.

3.2 Hybrid Shape Guidance

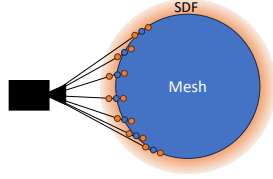
Our shape optimization is based on Score-Distillation Sampling (SDS) to distill gradients from a text prompt. The primary motivation to maintain an SDF representation in addition to the mesh is because SDFs are more robust to noisy guidance, which is an inherent property of the multi-view SDS approach (see Figure 3). We thus choose to inject the text guidance only to the auxiliary SDF representation and propagate the changes to the mesh via the consistency losses (Sec. 3.3) and the topology updates (Sec. 3.4).

To apply the text guidance and the consistency losses, we need to render both representation differentially. We use Nvdiffrast [Laine et al. 2020] to render meshes and VolSDF [Yariv et al. 2021] for volumetric rendering of our SDF. Clearly, as mesh rasterization is much

cheaper than volumetric rendering, the process is bottlenecked by the resolution at which we can render the SDF, both in terms of speed and memory. Our hybrid representation uniquely enables a strategy to render SDF faster and cheaper, at a higher resolution of 512x512.

This is achieved thanks to the consistency between the mesh and SDF representations throughout the optimization.

We can significantly reduce the typical 512 samples per ray necessary for rendering the SDF by using the intersection of the ray with the mesh representation (efficiently calculated by the differentiable mesh renderer). Using the intersection as the center of a small spread of samples (we use just 3 per ray), allows for high-resolution renders of the SDF (i.e., 512x512 and larger), which are otherwise memory prohibitive. The idea of leveraging the surface to reduce the number of network queries per ray emerged in concurrent works, namely Adaptive Shell [Wang et al. 2023b] and HybridNerf [Turki et al. 2024], which shows its generality and success in other settings than ours.



Using this strategy, we render the SDF in 512x512 and apply the VSD loss of those high-res renderings. We also apply regular SDS on lower-res 128x128 renderings by regular VolSDF as we find that this improves the results slightly.

3.3 Representation Priors

We apply representation-specific regularizations and consistency losses that keep both representations in sync.

Consistency Loss. The SDF and the mesh are consistent if their images are in 1 to 1 correspondences from any camera angle. We thus supervise the L2 difference between their RGB renderings and normal and opacity maps. If the renderings are made at different resolutions, we downsize to the lower resolution before the L2 loss.

Enforcing Localization and Freeze Loss. To localize changes to the user-selected area, we first fix the mesh vertices in all non-selected regions during optimization by zeroing out gradients outside of user selection. While localization is harder to achieve for SDF, we add a sampling-based freeze loss, which favors regions around fixed vertices to remain unchanged:

$$s(v_{\text{sampled}}) = 0 \quad (1)$$

where v_{sampled} are vertices sampled uniformly over the faces which are not part of the optimization region selected by the user.

Laplacian (Smoothness) Loss. While it is harder to regularize the surface of an implicit function to be smooth, the explicit representation of the mesh allows to easily define a smoothness term using the Laplacian of the mesh, inspired by [Kanazawa et al. 2018], defined for each vertex:

$$\delta(x_i) = x_i - \frac{\sum_{j=1}^N x_j}{N}, \quad (2)$$

where x_j are the N neighbors of x_i . The Laplacian vector encodes local curvature changes: a smooth mesh is defined by low Laplacian vectors. To encourage smoothness, we use a global loss:

$$L_{\text{smooth}} = \sum_i \|\delta(x_i)\|. \quad (3)$$

We opt for the uniform Laplacian instead of the cotan Laplacian, as the latter is more sensitive to ill-conditioned triangles, which may appear during the dynamic mesh updates.

SDF Eikonal Loss. To encourage the implicit function to learn a valid SDF representation, we use the Eikonal term as a loss [Gropp et al. 2020]. The SDF s is valid if and only if the loss in Eqn 4 is 0:

$$L_{\text{Eik}} = \sum_x (\|\nabla s(x)\| - 1)^2 \quad (4)$$

SDF opacity and normal Loss. Inspired by TextMesh [Tsalicoglou et al. 2024], we also binarize the SDF opacity and apply a Binary Cross Entropy loss to encourage discrete 0 or 1 values. To penalize badly oriented normals of the implicit surface, we apply an L2 penalty to the dot product between the normal and the camera direction if it is negative.

3.4 Updating the Mesh Topology

To maintain consistency between the mesh and SDF, it is necessary to perform local topology edits on the mesh in that increase or decrease mesh resolution where required. Continuous Remeshing [Palfinger 2022] pioneered such a local topology update approach by using the Adam optimizer state as a signal. While this approach works well in a multi-view reconstruction scenario, where the images are sharp and the camera parameters known, the noise involved in SDS makes the gradients, and by extension the Adam state, very noisy and unstable signal to trigger those operations. We turn to another work, ROAR [Barda et al. 2023], particularly well-tailored to our hybrid representation. Within this framework, we use the SDF as the signal to trigger mesh triangle splits.

In a nutshell, for each triangle on the mesh, ROAR starts by supersampling the triangle into K sub-faces, and projects each sub-vertices on the 0-level set of the SDF s using a projection operator:

$$P(x) = -s(x) \cdot \nabla s(x) \quad (5)$$

This projection results in a piece-wise linear surface that approximates the implicit surface closest to the initial triangle. The decision to split this triangle is based on the curvature score of this piece of projected surface. If the surface is very curved, then the triangle is split using $\sqrt{3}$ -subdivision [Kobbelt 2000]. Similarly, each edge is assigned a score based on the quadratic distance of its vertices to all the planes in the 1-ring of the edge, which intuitively represents how important the edge is to the geometry. If the score is low, then the edge can be collapsed with Qslim [Garland and Heckbert 2023].

We refer the interested reader to the ROAR paper [Barda et al. 2023] for more details, but the important point to note is that ROAR offers a principled way to perform edge collapses and face splits in the sense that each iteration of ROAR strictly decreases an energy - the difference between the highest face score and the lowest edge score. It thus exhibits a convergence behavior after enough iterations. We also note that manifoldness is guaranteed to be preserved throughout the iterations.

Average CLIP Score \uparrow	T2I	Implicit type	Appearance		Geometry	
			Implicit RGB	Implicit Normal	Mesh no texture Normal	
ProlificDreamer	SD2.1	NeRF	22.1	21.2	20.1	
HIFA	SD2.1	NeRF	23.2	23.1	22.0	
MVDreams	SD2.1	NeRF	25.9	25.4	24.1	
Fantasia3D	SD1.5	SDF	-	23.9	23.9	
TextMesh	DF	SDF	25.7	24.9	23.6	
Ours	DF	SDF	26.2	26.1	24.8	
¹ No high-res	DF	SDF	25.8	25.2	23.1	
² No low-res	DF	SDF	22.3	21.9	21.1	

Table 1. **Quantitative comparison on text-to-3D from scratch.** To validate our hybrid representation, we compare MagicClay with five state-of-the-art method for unconditional generation. We report the CLIP Score, *i.e.* the cosine similarity (scaled by 100) between prompt embeddings and 25 normal renders of the NeRFs/SDFs and texture-less meshes, taken in an equidistant circular pattern around the generated object, on a benchmark of 20 prompts, listed in the supplementary. We apply marching cubes to extract the meshes for NeRF-based methods, and isosurface extraction for SDF-based methods, except ours, as our dual representation already includes a mesh. For each method, we report the Text-to-Image model (T2I) used as a backbone : DeepFloyd (DF) or Stable-Diffusion (SD). We Note that Fantasia3D can not be run with DF, as it does not support diffusion in pixel-space. We validate that MagicClay has the highest Clip score for texture-less meshes, which can be verified qualitatively in Figure 4.

4 EXPERIMENTS

We implement our pipeline in Threestudio [Guo et al. 2023], and use DeepFloyd [StabilityAI 2023] as the backbone diffusion model. All experiments were executed on a single A100-40GB GPU. We provide further details, hyper-parameters, and additional examples of the texture maps generated by our method and the animation transfer application in the supplementary material.

In the rest of this section, we compare our representation to prior work on text-conditioned 3D generation (Sec. 4.1), demonstrate its utility in a mesh sculpting application (Sec. 4.2), and compare to a text-driven mesh deformation baseline (Sec. 4.3). We then provide a simple illustrative experiment to motivate the hybrid representation, and finally ablate our method (Sec. 4.5).

4.1 Comparison with Generative Methods

Since MagicClay is a modeling tool, we are primarily interested in evaluating the quality of the geometry and thus focus on mesh renderings without texture. Note that most existing 3D generative techniques are not designed to edit a part of an existing mesh, and therefore we start by comparing the performance of our hybrid approach for unconditional text-to-3D generation, seeking to establish the ability of our method to generate higher-quality meshes. We compare against five recent approaches: HIFA [Zhu and Zhuang 2024], MVDream [Shi et al. 2024], Fantasia3D [Chen et al. 2023], ProlificDreamer [Wang et al. 2023a] and TextMesh [Tsalicoglou et al. 2024]. We run the open-source implementation of all methods to produce results. We use Marching Cube to extract a mesh from NeRF-based methods, and isosurface extraction for SDF-based methods. We do not compare against Instant3D [Li et al. 2024] because they do not provide an implementation as of writing this

paper, but we note their ability to generate high-quality meshes. We measure the quality of the generated objects using an average clip score between the prompt and multi-view renderings. A complete description of our metric and the prompts used are given in the supplementary materials. We present our results in Figure 4 and Table 1. Extracted meshes often exhibit significant surface artifacts, which make them hardly recognizable without texture (see “Chow Chow puppy” by ProlificDreamer or “Croissant” by TextMesh). By comparison, our geometries are recognizable and smooth thanks to our hybrid representation enabling an explicit regularization of the surface. We further verify that, among competing approaches, MagicClay achieves the highest Clip Score between the prompts and texture-less renderings of the mesh. This shows that MagicClay achieves semantically meaningful reconstruction via geometry and not only texture, and thus successfully bridges the generative capabilities of implicit radiance fields with the surface-level controls of meshes.

Our hybrid representation is orthogonal to the choice of backbone text-to-image models. Fig 9 shows 3D models generated by MagicClay with SD 1.5, SD 2.1, and DeepFloyd, showing that the backbone model influences the quality of the results. This drives two conclusions : (1) improvements in the backbone translate into improvements for 3D generation. (2) In addition to the representation, an important differentiating factor for each method in Table 1 is the backbone, which we report.

4.2 Mesh Sculpting

MagicClay generates a modified mesh, which could be iteratively refined with new elements. Note that hybrid representation is essential to this application. Selecting the region of interest is easily accomplished by using standard mesh editing tools [Blender 2024]. Using the mesh allows us to keep non-selected surface regions intact by zeroing out their deformation gradients, which guarantees that the change will only affect the user-selected region. Because they are preserved, mesh properties can be transferred in the non-edited region, including texture, tessellation, and rigging parameters. Refer to Figures 1 for example results. MagicClay generates high-quality edits that match the rough local edit and adhere to the user’s text prompt.

4.3 Comparison with Contemporary 3D Editing Pipelines

A naive alternative to localized mesh sculpting would be to use the existing text-driven mesh deformation technique [Gao et al. 2023] and to zero-out the deformation field outside of the editing region, which is possible because the representation is explicit. We further compare with Latent-Nerf [Metzer et al. 2023] and Vox-E [Sella et al. 2023], but these approaches cannot guarantee a local edit because they are based on soft attention. We discuss Instruct-NeRF2NeRF [Haque et al. 2023] and DreamEditor [Zhuang et al. 2023] in supplementary

In Figure 8, we compare our method to these three baselines. Note how our method is able to add geometrically complex large-scale details due to guidance from SDF and topological updates. Our method’s changes are also restricted only to user-selected regions and do not lead to any changes in the other parts of the input.

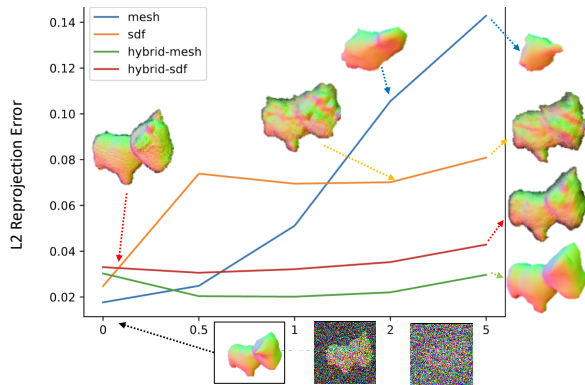


Fig. 3. **Mesh and SDF robustness to noisy gradients.** We optimize a **mesh**, an **SDF** and our hybrid representation with multi-view reconstruction losses after applying various noise levels to the ground truth renderings. We report the L2 reprojection error against novel-views ground truth renders. The SDF exhibits more robustness than the mesh to the high noise regime. We show the results for both the mesh (**hybrid-mesh**) and SDF (**hybrid-SDF**) in our hybrid representation. The **hybrid-mesh** significantly outperforms the **mesh** only baseline in the high noise regime.

4.4 Analysis of Mesh and SDF Robustness to Noise

We now motivate the use of our hybrid representation by a simple controlled experiment, where we aim to reconstruct a fixed 3D target with different levels of noise in the guidance. Even though we use synthetic noise, we expect these findings to apply in an SDS setting, where gradients are noisy due to the noising step performed at each SDS iteration [Poole et al. 2023].

Given multi-view renderings of a fixed ground truth 3D model, we add uncorrelated per-pixel Gaussian noise to each image and compute L2 pixel-wise loss to guide our shape representation towards the target. A complete overview of the experiment setup is given in the supplementary materials. As we increase the noise level (by increasing standard deviation) we find that different representations are more prone to errors in reconstructing the target. We use L2 re-projection error with respect to the ground truth shape on novel views as our evaluation metric, and compare vanilla Mesh, SDF representations to our hybrid approach (using both SDF and mesh renderings), and show results in Figure 3. At the highest noise regimes (standard deviation of 5), the mesh reconstruction degenerates to a blob, while the SDF reconstruction is still recognizable despite surface irregularities. Importantly, the hybrid representation performs better than both individual representations at all levels of noise, and the benefits are the strongest at higher noise levels. The hybrid-SDF outperforms the SDF baseline because the mesh acts as a regularizer for more 3D consistency. The L2 reprojection loss of the hybrid-mesh is lower than the hybrid-SDF because the SDF tends to exhibit a “haze” artifacts throughout the entire image, including the background pixels, while the mesh rendering can not create this effect in the background, serving as a sort of regularization on its own. Finally, we note that all curves are not strictly increasing,

which we attribute to the fact that we test on novel views: some amount of noise may prevent overfitting to the training views.

Note that this experiment is not designed to claim superiority of the hybrid representation over the SDF, but rather to show its robustness to noise.

4.5 Ablations

512x512 SDF renderings. We show in Figure 6 and Table 1 that high-resolution SDF rendering significantly affects generated shape quality. This shows that the mesh part of the hybrid helping to accelerate SDF rendering plays a role in quality.

Initial editing. In our experiments, only significant differences in the initial sculpt lead to different generated results. Typically, performing an initial sculpt does impact the result compared to just selecting a region with no sculpting. However, two initial sculpts that are similar will lead to the same final results (see Figure 10).

Not enforcing localization, no freeze loss. We remove the mechanism for enforcing localization via fixing non-selected surface regions and nearby SDF values as discussed in Sec. 3.3. In Figure 11, The shapes undergo unintended global changes, potentially erasing the original shape.

No topology updates. The topological updates (Sec. 3.4) allow to add resolution gradually. Optimizing a fixed-resolution mesh would either result in a shape that only marginally differs from the input if the initial resolution is too high or lacks fine details if the initial resolution is too coarse (Figure 5). These results complement, in a generative setting, the experiments of [Palfinger 2022]¹, performed with ground truth multi-view supervision which similarly shows that optimizing very high-poly meshes leads to local minima.

5 CONCLUSION

We presented MagicClay, a generative sculpting tool backed by our new hybrid SDF and mesh representation. Key to the success of the generative process is our new rendering strategy that leverages the mesh part of the hybrid representation to localize ray sampled in the volumetric rendering of the SDF. We believe MagicClay is an important step towards turning the recent advancements in text-to-image-from-scratch into an actual modeling tool usable by artists in an iterative workflow.

Limitations. Our method is inherently constrained by the quality of the SDS gradients. Each view tracts the optimization in a different direction adding noise and rendering the emergence of fine details more difficult. Second, MagicClay is not interactive, *e.g.* running MagicClay takes 1 hour per prompt on an A100 GPU, with the bottleneck being the SDS loss

Future work. We see opportunities to leverage inpainting and depth-conditioned diffusion models to speed up the convergence of SDS. Indeed, this generative process transforms the full object in each rendering, whereas it is clear that some parts of the generated image should stay the same as the 3D edit is localized. We think that leveraging this insight would reduce the amount of noise inherent in SDS.

¹We refer the reader to the videos in the Readme of their GitHub repository

REFERENCES

- Autodesk. 2024. Mudbox. <https://www.autodesk.com/products/mudbox>. (2024).
- Amir Barda, Yotam Erel, Yoni Kasten, and Amit H. Bermano. 2023. ROAR: Robust Adaptive Reconstruction of Shapes Using Planar Projections. (2023). arXiv:2307.00690 [cs.GR]
- Henning Biermann, Ioana Martin, Fausto Bernardini, and Denis Zorin. 2002. Cut-and-Paste Editing of Multiresolution Surfaces. *SIGGRAPH* (2002).
- Blender. 2024. <http://www.blender.org>. (2024).
- Hansheng Chen, Ruoxi Shi, Yulin Liu, Bokui Shen, Jiayuan Gu, Gordon Wetzstein, Hao Su, and Leonidas Guibas. 2024. Generic 3D Diffusion Adapter Using Controlled Multi-View Editing. *arXiv preprint 2403.12032* (2024).
- Rui Chen, Yongwei Chen, Ningxin Jiao, and Kui Jia. 2023. Fantasia3D: Disentangling Geometry and Appearance for High-quality Text-to-3D Content Creation. (2023).
- Zhiqin Chen and Hao Zhang. 2019. Learning Implicit Fields for Generative Shape Modeling. *CVPR* (2019).
- Xinhua Cheng, Tianyu Yang, Jianan Wang, Yu Li, Lei Zhang, Jian Zhang, and Li Yuan. 2024. Progressive3D: Progressively Local Editing for Text-to-3D Content Creation with Complex Semantic Prompts. arXiv:2310.11784 [cs.CV] <https://arxiv.org/abs/2310.11784>
- Thomas Funkhouser, Michael Kazhdan, Philip Shilane, Patrick Min, William Kiefer, Ayellet Tal, Szymon Rusinkiewicz, and David Dobkin. 2004. Modeling by Example. *ACM Transactions on Graphics* (2004).
- William Gao, Noam Aigerman, Thibault Groueix, Vladimir G. Kim, and Rana Hanocka. 2023. TextDeformer: Geometry Manipulation using Text Guidance. *SIGGRAPH* (2023).
- Michael Garland and Paul S. Heckbert. 2023. Surface Simplification Using Quadric Error Metrics. *Seminal Graphics Papers: Pushing the Boundaries* (2023).
- Amos Gropp, Lior Yariv, Niv Haim, Matan Atzmon, and Yaron Lipman. 2020. Implicit geometric regularization for learning shapes. *ICML* (2020).
- Yuan-Chen Guo, Ying-Tian Liu, Ruizhi Shao, Christian Laforte, Vikram Voleti, Guan Luo, Chia-Hao Chen, Zi-Xin Zou, Chen Wang, Yan-Pei Cao, and Song-Hai Zhang. 2023. ThreeStudio: A unified framework for 3D content generation. <https://github.com/threestudio-project/threestudio>. (2023).
- Ayaan Haque, Matthew Tancik, Alexei Efros, Aleksander Holynski, and Angjoo Kanazawa. 2023. Instruct-NeRF2NeRF: Editing 3D Scenes with Instructions. In *ICCV*.
- Alec Jacobson, Zhigang Deng, Ladislav Kavan, and J.P. Lewis. 2014. Skinning: Real-time Shape Deformation. *ACM SIGGRAPH Course* (2014).
- Evangelos Kalogerakis, Siddhartha Chaudhuri, Daphne Koller, and Vladlen Koltun. 2012. A Probabilistic Model of Component-Based Shape Synthesis. *ACM Transactions on Graphics* 31, 4 (2012).
- Angjoo Kanazawa, Shubham Tulsiani, Alexei A Efros, and Jitendra Malik. 2018. Learning category-specific mesh reconstruction from image collections. (2018).
- Leif Kobbelt. 2000. Sqrt(3)-Subdivision. *ACM SIGGRAPH* (2000).
- Samuli Laine, Janne Hellsten, Tero Karras, Yeongho Seol, Jaakko Lehtinen, and Timo Aila. 2020. Modular Primitives for High-Performance Differentiable Rendering. *ACM Transactions on Graphics* 39, 6 (2020).
- Jiahao Li, Hao Tan, Kai Zhang, Zexiang Xu, Fujun Luan, Yinghao Xu, Yicong Hong, Kalyan Sunkavalli, Greg Shakhnarovich, and Sai Bi. 2024. Instant3D: Fast text-to-3D with sparse-view generation and large reconstruction model. *ICLR* (2024).
- Yuhan Li, Yishun Dou, Yue Shi, Yu Lei, Xuanhong Chen, Yi Zhang, Peng Zhou, and Bingbing Ni. 2023. FocalDreamer: Text-driven 3D Editing via Focal-fusion Assembly. arXiv:2308.10608 [cs.CV] <https://arxiv.org/abs/2308.10608>
- Chen-Hsuan Lin, Jun Gao, Luming Tang, Towaki Takikawa, Xiao-hui Zeng, Xun Huang, Karsten Kreis, Sanja Fidler, Ming-Yu Liu, and Tsung-Yi Lin. 2023. Magic3D: High-Resolution Text-to-3D Content Creation. *CVPR* (2023).
- Gal Metzger, Elad Richardson, Or Patashnik, Raja Giryes, and Daniel Cohen-Or. 2023. Latent-NeRF for Shape-Guided Generation of 3D Shapes and Textures. *CVPR* (2023).
- Aryan Mikaeili, Or Perel, Mehdi Safaei, Daniel Cohen-Or, and Ali Mahdavi-Amiri. 2023. SKED: Sketch-guided Text-based 3D Editing. *ICCV* (2023).
- Ben Mildenhall, Pratul P Srinivasan, Matthew Tancik, Jonathan T Barron, Ravi Ramamoorthi, and Ren Ng. 2020. Nerf: Representing scenes as neural radiance fields for view synthesis. *ECCV* (2020).
- Thomas Müller, Alex Evans, Christoph Schied, and Alexander Keller. 2022. Instant Neural Graphics Primitives with a Multiresolution Hash Encoding. *ACM Transactions on Graphics* (2022).
- Werner Palfinger. 2022. Continuous remeshing for inverse rendering. *Computer Animation and Virtual Worlds* (2022).
- Jeong Joon Park, Peter Florence, Julian Straub, Richard Newcombe, and Steven Lovegrove. 2019. DeepSDF: Learning Continuous Signed Distance Functions for Shape Representation. *CVPR* (2019).
- Mengqi Peng, Jun Xing, and Li-Yi Wei. 2018. Autocomplete 3D Sculpting. *ACM SIGGRAPH* (2018).
- Ben Poole, Ajay Jain, Jonathan T. Barron, and Ben Mildenhall. 2023. DreamFusion: Text-to-3D using 2D Diffusion. *ICLR* (2023).
- Omid Poursaeed, Matthew Fisher, Noam Aigerman, and Vladimir G. Kim. 2020. Coupling Explicit and Implicit Surface Representations for Generative 3D Modeling. (2020).
- Guocheng Qian, Jinjie Mai, Abdullah Hamdi, Jian Ren, Aliaksandr Siarohin, Bing Li, Hsin-Ying Lee, Ivan Skorokhodov, Peter Wonka, Sergey Tulyakov, and Bernard Ghanem. 2024. Magic123: One Image to High-Quality 3D Object Generation Using Both 2D and 3D Diffusion Priors. *ICLR* (2024).
- Marie-Julie Rakotosaona, Fabian Manhardt, Diego Martin Arroyo, Michael Niemeyer, Abhijit Kundu, and Federico Tombari. 2024. NeRFMeshing: Distilling Neural Radiance Fields into Geometrically-Accurate 3D Meshes. *3DV* (2024).
- Gabriele Salvati, Christian Santoni, Valentina Tibaldo, and Fabio Pellacini. 2015. Mesh-Histo: Collaborative Modeling by Sharing and Retargeting Editing Histories. *ACM Transactions on Graphics* (2015).
- R Schmidt, C Grimm, and B Wyvill. 2006. Interactive decal compositing with discrete exponential maps. *ACM SIGGRAPH* (2006).
- Etai Sella, Gal Fiebelman, Peter Hedman, and Hadar Averbuch-Elor. 2023. Vox-E: Text-guided Voxel Editing of 3D Objects. *CVPR* (2023).
- Tianchang Shen, Jun Gao, Kangxue Yin, Ming-Yu Liu, and Sanja Fidler. 2021. Deep Marching Tetrahedra: a Hybrid Representation for High-Resolution 3D Shape Synthesis. *NeurIPS* (2021).
- Yichun Shi, Peng Wang, Jianglong Ye, Mai Long, Kejie Li, and Xiao Yang. 2024. MV-Dream: Multi-view Diffusion for 3D Generation. *ICLR* (2024).
- StabilityAI. 2023. DeepFloyd IF: a novel state-of-the-art open-source text-to-image model with a high degree of photorealism and language understanding. <https://www.deepfloyd.ai/deepfloyd-if>. (2023). Retrieved on 2023-11-08.
- SubstanceModeler. 2024. Substance Modeler. <https://www.adobe.com/ie/products/substance3d-modeler.html>. (2024).
- Christina Tsalicoglou, Fabian Manhardt, Alessio Tonioni, Michael Niemeyer, and Federico Tombari. 2024. TextMesh: Generation of Realistic 3D Meshes From Text Prompts. *3DV* (2024).
- Haithem Turki, Vasu Agrawal, Samuel Rota Bulò, Lorenzo Porzi, Peter Kotschieder, Deva Ramanan, Michael Zollhöfer, and Christian Richardt. 2024. HybridNeRF: Efficient Neural Rendering via Adaptive Volumetric Surfaces. *CVPR* (2024).
- Zhengyi Wang, Cheng Lu, Yikai Wang, Fan Bao, Chongxuan Li, Hang Su, and Jun Zhu. 2023a. ProlificDreamer: High-Fidelity and Diverse Text-to-3D Generation with Variational Score Distillation. *NeurIPS* (2023).
- Zian Wang, Tianchang Shen, Merlin Nimier-David, Nicholas Sharp, Jun Gao, Alexander Keller, Sanja Fidler, Thomas Müller, and Zan Gojcic. 2023b. Adaptive Shells for Efficient Neural Radiance Field Rendering. *ACM Transactions on Graphics*, Article 259 (2023).
- Lior Yariv, Jiatao Gu, Yoni Kasten, and Yaron Lipman. 2021. Volume rendering of neural implicit surfaces. (2021).
- Cem Yuksel, John Keyser, and Donald House. 2010. Mesh Colors. *ACM Transactions on Graphics* (2010).
- Ersin Yumer, Siddhartha Chaudhuri, Jessica Hodgins, and Levent Burak Kara. 2015. Semantic Shape Editing Using Deformation Handles. *SIGGRAPH* (2015).
- ZBrush. 2024. <https://www.maxon.net/en/zbrush>. (2024).
- Junzhe Zhu and Peiye Zhuang. 2024. HiFA: High-fidelity Text-to-3D Generation with Advanced Diffusion Guidance. *ICLR* (2024).
- Jingyu Zhuang, Chen Wang, Lingjie Liu, Liang Lin, and Guanbin Li. 2023. DreamEditor: Text-Driven 3D Scene Editing with Neural Fields. *SIGGRAPH Asia* (2023).

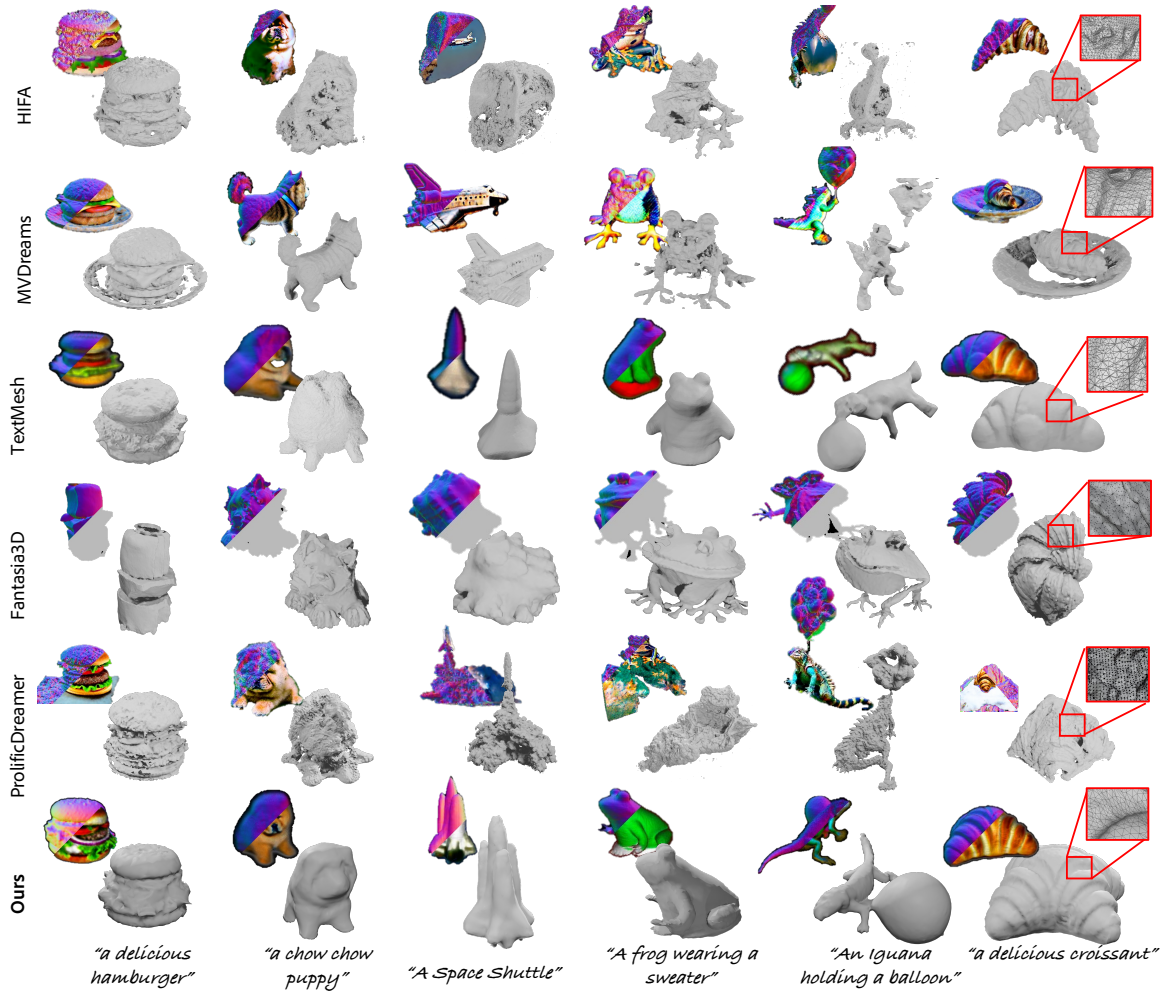


Fig. 4. **Qualitative comparison on text-to-3D from scratch.** To validate the benefit of our hybrid approach, we compare the quality of the triangular meshes extracted from HIFA [Zhu and Zhuang 2024], MVDreams [Shi et al. 2024], TextMesh [Tsalicoglou et al. 2024], Fantasia3D [Chen et al. 2023] and ProlificDreamer [Wang et al. 2023a]. For each prompt and method, we show the normal and RGB rendering on the top left, and the textureless mesh on the bottom right. While all methods produce realistic RGB renderings, only our hybrid representation generates smooth geometry, as highlighted by the red insets.

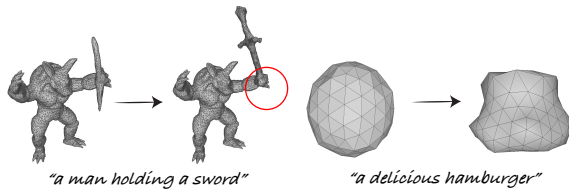


Fig. 5. **Ablation: no topology updates.** Optimizing the mesh without topology update results in the final generated object being limited by the initial resolution. **Left** When starting with a fine mesh the optimization will often get stuck since each vertex has tiny effect on the objective: notice the sword is unable to grow its tip. **Right** When starting from a coarse mesh, no fine details can be created.

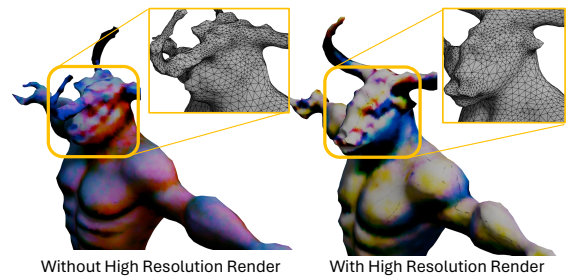


Fig. 6. **Ablation on high resolution renderings.** Without our scheme to render SDF in high resolution by using the mesh counter part to localize samples along the ray, we default to regular low resolution SDS on the SDF renderings, leading to poorer quality in the generated shapes.

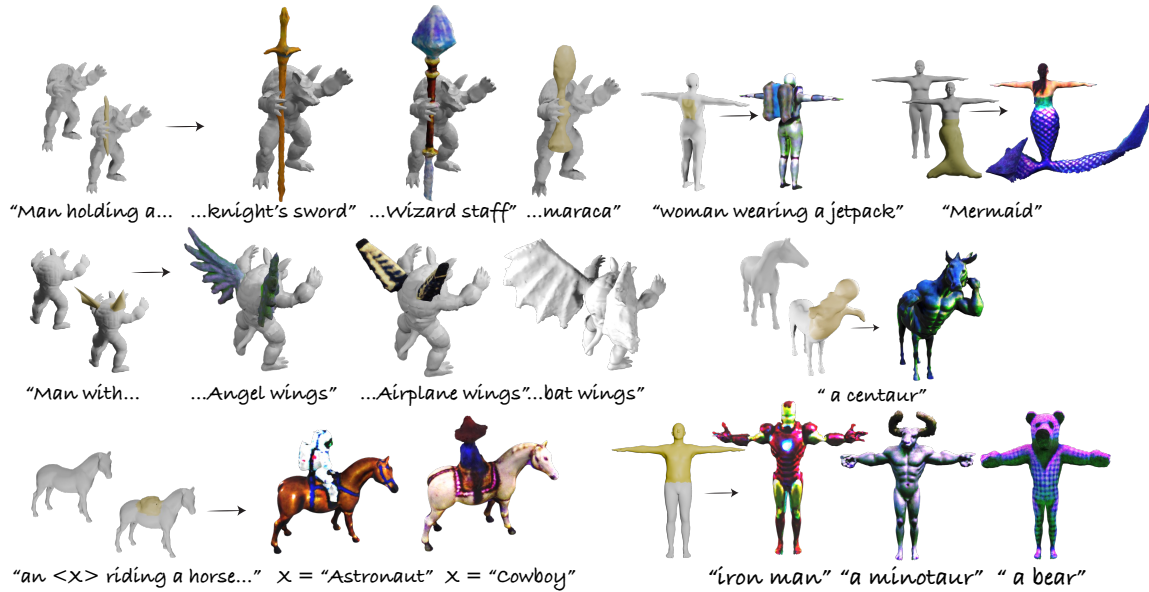


Fig. 7. **Sculpting gallery.** *Left:* from a source mesh, the user performs a rough edit in under two minutes, highlighted in yellow. *Right:* MagicClay’s output.

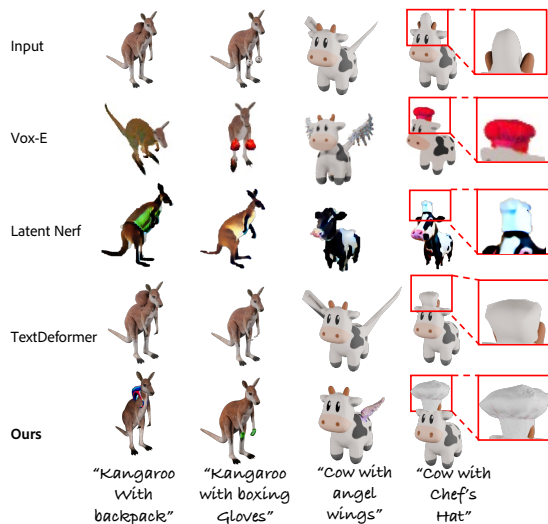


Fig. 8. **Comparisons to other 3D-editing approaches.** We compare MagicClay with other generative approaches able to edit meshes [Sella et al. 2023; Metzger et al. 2023]. Note that the baselines *do not* strictly preserve the non-editing region and texture. They rely on soft attention, which leads in some cases to the inadvertent destruction of features such as the cow’s horns. In contrast, our method is guaranteed to be non destructive for the existing geometry and preserves its texture. We post-process TextDeformer [Gao et al. 2023] to support localized edits, and show that the space of deformation it can achieve is less expressive.



Fig. 9. **Varying the backbone of MagicClay.** We show that MagicClay is orthogonal to the backbone text-to-image model used to provide gradients in Score-Distillation Sampling. We observe a quality and required VRAM trade off for various models.



Fig. 10. **Robustness to the initial edit.** MagicClay sculpts the hat from various levels of manual initialization. We find that similar initial edits give similar results (middle and right). No edit or small edits (left) lead to smaller changes, after the allocated 10k iterations. Note that MagicClay is *not* invariant w.r.t. the initial edit, as it is not desirable in a sculpting workflow.

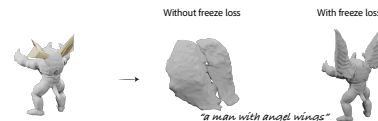


Fig. 11. **Ablation: no localization.** W/o localization and freeze losses, shape changes can propagate beyond the user-selected area, potentially destroying the initial content. Here, armadillo is erased by “angel wings.”